PHYSICAL REVIEW C, VOLUME 60, 021601

Preequilibrium emission observed in the correlation between light particles and evaporation residues for the $^{84}Kr+^{27}Al$ system

J. Gómez del Campo,[1] D. Shapira,[1] J. McConnell,[1] C. J. Gross,[1,2] D. W. Stracener,[3] H. Madani,[1,*] E. Chávez,[4] and M. E. Ortíz[4]

[1]*Physics Division, Oak Ridge National Laboratory, Oak Ridge, Tennessee 37831*

[2]*Oak Ridge Institute for Science and Education, Oak Ridge, Tennessee 37831*

[3]*University of Tennessee, Knoxville, Tennessee 37996*

[4]*Instituto de Física Universidad Nacional Autónoma de México, México 01000 Distrito Federal, México*

(Received 24 August 1998; published 7 July 1999)

Evaporation residues (ER) of $Z=34-42$ were measured in coincidence with emitted protons, deuterons, tritons, and α particles for the reaction $^{84}Kr+^{27}Al$ at a ^{84}Kr bombarding energy of 1260 MeV. Our study demonstrates the presence of a strong preequilibrium component in the reaction yield. The assumption of a forward center-of-mass angular distribution for the emission of energetic protons and α, following full momentum transfer, gives the best description of the observed experimental data. This description differs substantially from the one provided by prevailing models of incomplete fusion. [S0556-2813(99)50108-8]

PACS number(s): 25.70.Jj

In heavy-ion nuclear collisions above 10 MeV/nucleon, the process of complete fusion (CF) and equilibrium decay begins to fail and mechanisms such as incomplete fusion (IF) and preequilibrium emission occurs. During the past two decades [1–7], some understanding of IF reactions and preequilibrium emission has been reached; however, a full understanding of the mechanisms, primarily those associated with the loss of particles prior to equilibration, still eludes us. Frequently, the term incomplete momentum transfer has been employed [3,5] to indicate that, somehow, particles are lost from the target and/or projectile before fusion of the remnants occurs. This conclusion has been supported primarily by inclusive measurements of the energy and/or velocity spectra of ER-like fragments [1–5] or folding angles in the case of fusion and fission [6]. Coincidence measurements between ER and light-charged particles have been done in a few cases [5,7] but in these studies, the nucleons emitted at forward angles (laboratory angles smaller than 11°) escape detection. The general conclusion from such studies is that the data are consistent with particles lost from the lighter of the reactants. In our studies we use inverse kinematics (heavy projectile on light target) so that the ER possess a high recoil velocity that allows for complete measurements and particle identification through E-ΔE and/or time-of-flight techniques [2,8]. In cases where the mass of the projectile is not far removed from that of the ER, the overlap with projectilelike reactions such as deep inelastic collision (DIC) can be an important component which needs to be addressed, especially at bombarding energies above 10 MeV/nucleon.

Unique aspects of the present measurements are complete detection and identification *(Z)* of the ER and complete kinematic measurements of coincident light particles, protons *(p)*, deuterons *(d)*, tritons *(t)*, and alphas (α), in a 25° cone centered around the beam excluding the angles from 0° to 2.5° that allow the beam to go through the detector stopping in a Faraday cup located behind. With these data, a clear separation between ER and products of DIC and quasielastic reactions was achieved. The principal observation is that bulk preequilibrium particle emission occurs from the composite system after full stopping of the projectile, in contrast with observations and published systematics [2,4] (obtained from inclusive measurements).

The experiment was carried out using the large detector array HILI [9]. This detector system was used in previous measurements of similar reactions leading to compound nuclei with $A\sim100$ [10–12]. We emphasize here that the detector system covered an angular range of 2.5° to 25°. The ER were detected in an ionization chamber and the coincident light particles were detected and identified by a high-granularity array of plastic ''Phoswich'' [13] scintillation counters placed behind the ionization chamber. The beam of ^{84}Kr at 1260 MeV was extracted from the Texas A&M University Superconducting Cyclotron. Timing between the Cyclotron's rf and the hodoscopes was used to separate the $Z=1$ particles by time of flight.

The measured energy spectra of ER of $Z=39$, 40, and 41 are shown in Fig. 1 by the crosses. These spectra have a trigger condition of $m\geqslant1$, where m is the charged-particle (p, d, t, and α) multiplicity measured by the HILI and have been integrated over the laboratory angle from 2.5° to 25°. Plotted on the vertical axis is the differential multiplicity (dM/dE) defined as the ratio of the counts of a given residue in the energy bin dE (2 MeV steps) to the total ER counts (integrated over angle, energy, and Z for $Z\geqslant39$). The other spectra shown in Fig. 1 are results from calculations that will be discussed later on. The experimental centroids (in MeV) of the ER were extracted from spectra such as those shown in Fig. 1 and are plotted in Fig. 2 for all fragments from $Z=34$ to 42. The solid points are the experimental centroids corresponding to the inclusive measurements (singles). The open squares correspond to centroids extracted from ER energy spectra with the multiplicity condition m

*Present address: Research and Data Systems Corporation, Seabrook, MD 20706.

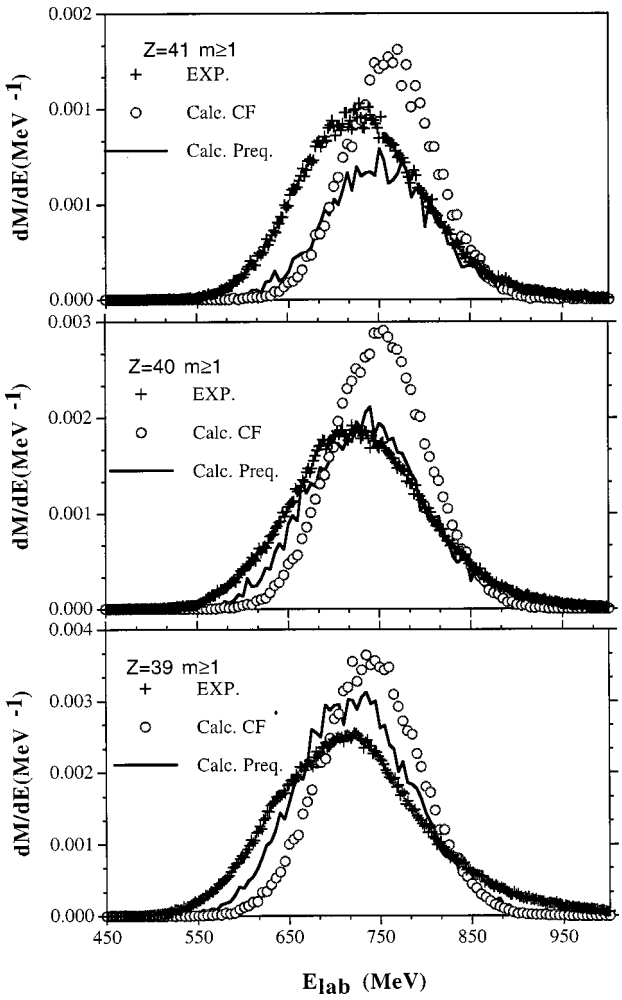

FIG. 1. Experimental (crosses) energy spectra of $Z=41$, 40, and 39 ions compared to statistical model calculations (open circles) and preequilibrium calculations (solid curves) for ER products of ^{84}Kr+^{27}Al at ^{84}Kr=1260 MeV.

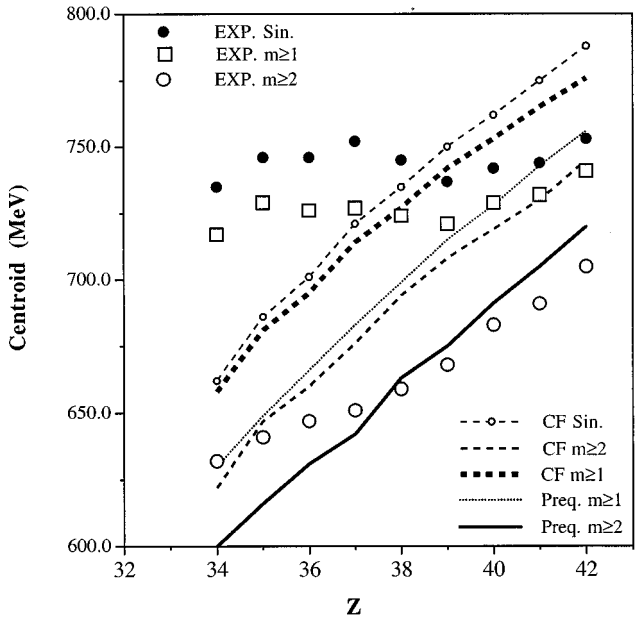

FIG. 2. Experimental centroids of the energy spectra. The solid circles correspond to the singles measurements, the open squares to those obtained with $m\geqslant 1$ and the open circles to those with $m\geqslant 2$. The various curves are calculations described in the text and labeled in the figure. m refers to the light-charged-particle multiplicity measured by the detector.

$\geqslant 1$ and the open circles are those for $m\geqslant 2$. The main observation to point out from Fig. 2 is the large difference in the slope of the data of centroid vs Z when changing from singles and $m\geqslant 1$ to $m\geqslant 2$. A qualitative explanation of this effect is that the spectra, for Z around and below the beam ($Z=36$), contain substantial contributions from projectile-like processes. In fact, a comparison of the widths of the energy spectra (for the singles or $m<1$) for Z from 34 to 40 reveals that those of $Z<38$ are wider by about a factor of 2 in respect to those of $Z\geqslant 38$ indicating that the contribution arising from two bodylike reactions (such as DIC and quasi-elastic reactions) are very strong for Z values at or close to that of the beam ($Z=36$). The width analysis for the spectra of $m>2$ shows that the width values for $Z>34$ are all very similar within 30% indicating that the contributions arising from two bodylike reactions are reduced significantly because they have lower particle multiplicities than the CF reaction.

A more quantitative analysis of the data displayed in Fig. 2 requires detailed modeling of the CF reaction and equilibrium decay. This was done using the code LILITA [14]. The statistical model parameters used are similar to those employed in the description of the fusion reactions given in Refs. [10–12]. Maximum critical angular momentum values of $63\hbar$ [10,11] and a level density parameter $a=A/12$ were used for the compound nucleus. These Monte Carlo simulations had all the experimental constraints (geometry, threshold, efficiency) folded in (see Ref. [12]). The resulting energy spectra are shown in Fig. 1 (open circles) for the ER of $Z=39$, 40, and 41. As can be seen from the comparisons to the data, the predicted energy spectra for $Z=40$ and 41 have centroids that are higher and widths that are smaller than the experimental ones. This behavior is opposite from that expected from published systematics of IF [2,4]. According to this systematics, particles should be lost from the target (^{27}Al) causing a shift of the centroids to higher energies. The predicted centroids for CF depend only on the full momentum transfer assumption and on the fact that the equilibrium emission of the light particles is symmetric with respect to 90° cm in the frame of the emitting compound nucleus. Therefore, the usual uncertainties in the statistical model parameters (like level densities and transmission coefficients) have no effect on the discussion of the centroids of the energy spectra presented in Fig. 2.

Inspecting our results for the centroids given in Fig. 2 as a function of the Z of the ER, one sees a rather interesting effect. The small circle-dashed line and the thick-dashed line drawn in Fig. 2 correspond to the centroids extracted from simulations of the CF case for the singles and the $m\geqslant 1$ conditions, respectively. As can be seen, the experimental centroids are higher than the calculations for all Z values

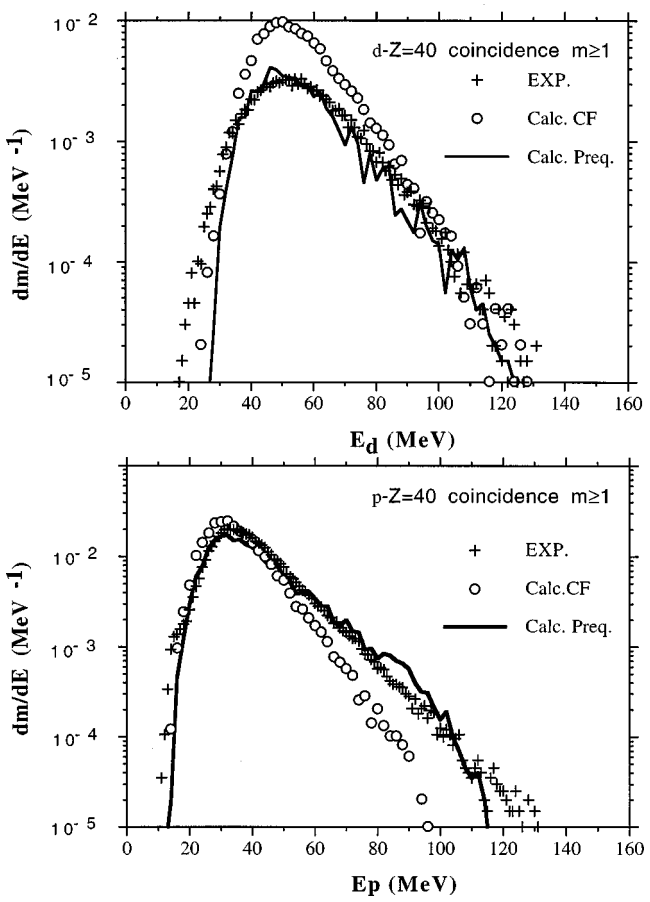

FIG. 3. Experimental energy spectra (crosses) of d (top panel) and p (bottom panel) in coincidence with $Z=40$. The calculations are (open circles) for complete fusion and solid curves for preequilibrium mechanisms.

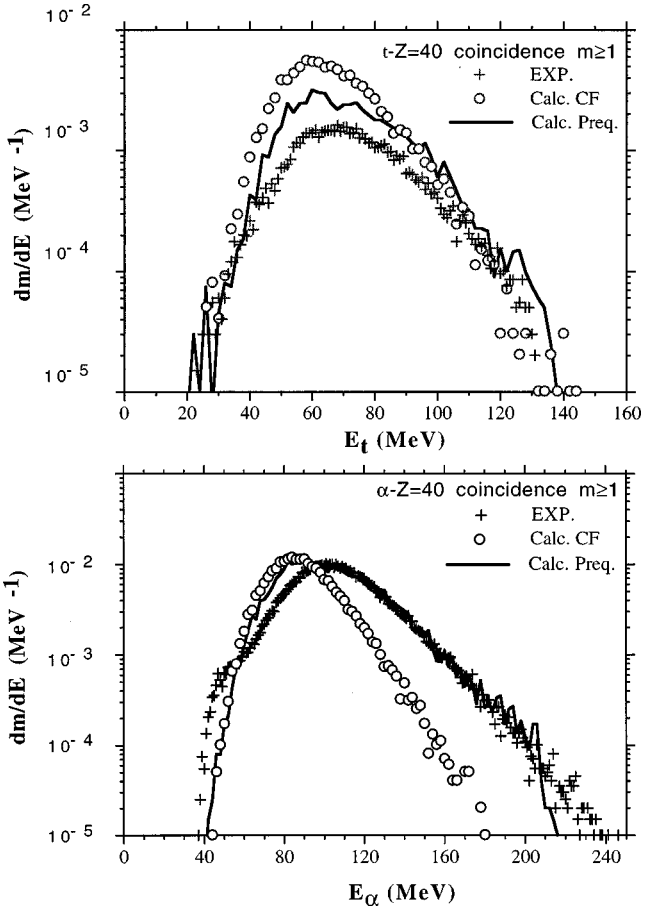

FIG. 4. Experimental energy spectra (crosses) of t (top panel) and α (bottom panel) in coincidence with $Z=40$. The calculations are (open circles) for complete fusion and solid curves for preequilibrium mechanisms.

below $Z=37$, apparently consistent with the idea of IF systematics. However, when the comparisons are made for the $m\geqslant 2$ case (which preferentially selects the ER components in the energy spectra) one can see that *all* the experimental centroids (except $Z=34$) are much *lower* than the CF prediction for $m\geqslant 2$ (thin-dashed line in Fig. 2). This apparent agreement with the IF systematics, seen for the centroids below $Z=37$ (for singles and $m\geqslant 1$), is then due to the fact that DIC and quasielastic components included in the experimental data shift the centroids to higher energies. We suggest that many other analyses made at similar bombarding energies [2,4], where only inclusive data were measured and mostly the spectra for Z at or below that of the beam were analyzed, the contamination with projectilelike fragments has obscured the real picture. The remaining point in this discussion is to understand the difference between the experimental centroids of what we consider filtered ER yields (open circles) and the CF calculations (thin-dashed curve). To accomplish this we first turn to the analysis of the emitted light-particle spectra.

In Fig. 3 we show the experimental energy spectra (crosses) of p and d in coincidence with ER of $Z=40$ and in Fig. 4 for those of t and α. The trigger condition $m\geqslant 1$ means that at least one light-charged particle (including the one whose spectrum is given in Figs. 3 or 4) is in coincidence with $Z=40$. The spectra have been summed over laboratory angles from 2.5° to 25°. On the vertical scale is the differential multiplicity dm/dE defined as the number of counts of the selected particle detected divided by the total number of $Z=40$ fragments detected. The simulations for CF are shown by the open circles in Figs. 3 and 4 using the same definition for the differential multiplicity. As can be seen from the comparisons given in Figs. 3 and 4, there is a very large difference between simulated and experimental spectra for p and α, primarily in the behavior of the high-energy component. Also, it should be noted that the multiplicity predicted is higher for d and t (this effect is also present at lower energies [10–12]). The largest discrepancy between the experiment and the CF calculations exists for the α particle spectra (see Fig. 4, bottom panel).

One appealing explanation for the high-energy excess of α and p is that of precompound decay of the kind discussed by several authors [15–17]. It should be noticed that the excess of high-energy p or α's cannot be explained as projectilelike emission since these would contribute around 15 MeV/nucleon (i.e., 15 MeV p and 60 MeV α's). Also, emissions from target breakup will be much lower in energy. We modeled the preequilibrium decay using the code RELAX

[15], which was used previously by the authors of Ref. [18] for higher bombarding energies. The preequilibrium particle decay occurs form a source moving at the composite of target and projectile velocity and is then followed by equilibrium decay using the code LILITA. The code RELAX calculates only *p* and *n* emission and, as can be seen from the data of Fig. 4, the main effect is on the α's. Therefore, the procedure used was to calculate from RELAX (with the input parameters given in Ref. [15]) only the energy spectra of *p* and *n* in the center-of-mass system (c.m.) and then scale them to the α's, assuming equal velocities. The relative probability for α, *p*, and *n* in this first step was chosen as 50%, 25%, and 25%, respectively. The angular distribution (in the c.m.) of the emitted particles was of the form $\exp(-\theta/\Delta\theta)$ with $\Delta\theta = 10°$. In the philosophy of the preequilibrium model, the energy spectrum of the emitted nucleons depends on the total excitation energy of the composite system (295 MeV for the present case). With these parameters, allowing for two preequilibrium decay steps followed by equilibrium emission (using LILITA), we obtain the results shown in Figs. 3 and 4 (solid lines labeled Calc. Preq.). The proton spectrum (bottom panel of Fig. 3) is well reproduced as well as the high-energy part of the α spectrum. For low-energy α's, the calculation predicts too much yield. The source of this discrepancy is in the equilibrium decay simulation part of the cascade, and has been discussed in previous publications [10,12]. It should also be noticed that the fit for the *d* spectra is very good (the multiplicity came down as a result of not allowing preequilibrium *d* emission in the first two steps). Also the *t* multiplicity came down significantly, producing a much better description of the spectrum. In Ref. [7], it was also noted that the preequilibrium contribution from *d* and *t* was about a factor of 10 lower than that for *n*, *p*, and α. A detailed theoretical description of the dissipation mechanism responsible for the precompound emission strength and kinematics is not available. Also, current models do not address the preequilibrium emission of clusters such as *d*, *t*, and α. In the preequilibrium calculations presented here, the assumptions that were made and already discussed were done with the sole purpose of demonstrating how the preequilibrium mechanism could account for the detailed exclusive data obtained for the $^{84}Kr + ^{27}Al$ system. Also, it is important to emphasize that current models of IF do not explain the data.

The effect of precompound emission on the simulated ER spectra are displayed in Fig. 1 (solid lines). The fit in multiplicity and shape is excellent for $Z = 40$ and a little off for $Z = 41$ and 39. The change in dM/dE with respect to the CF calculations (open points) is due mostly to the spread on the width of the spectra because of the higher recoil energy given to the ER due to the energetic emission of the light particles. The downward shift of the centroid in these stimulated spectra is a consequence of the forward peaked angular distribution stipulated for the precompound emission of *p*, *n*, and α's. Preequilibrium emission from the composite system (i.e., after full momentum transfer) accounts for both the high-energy component in the emission of *p* and α and downward shift are observed in the centroid of the ER energy distribution. Finally, Fig. 2 shows that precompound emission, as stipulated here, reproduces the trend in ER energy distribution. The drastic change in the calculated result for CF $m \geqslant 2$ and Preq. $m \geqslant 2$ attests to the important role preequilibrium emission has in these reactions.

In conclusion, our results indicate that a process of preequilibrium emission of energetic light particles (*n*, *p*, α) from the composite system peaked in the direction of the incident beam can account for both ER and light-particle emission spectra and relative multiplicities in $^{84}Kr + ^{27}Al$ at 15 MeV/nucleon. In addition, we find in our analysis that there is no need to refer explicitly to particles lost from the target or projectile and results should depend mostly on the total excitation energy deposited in the composite system. The results for reactions involving direct kinematics (for instance, those of Refs. [1, 3, 5, 6] are all consistent with these preequilibrium pictures; however, those involving inverse kinematics [2,4] are not. The explanation for these inconsistencies could be due to contamination with DIC reactions on the projectile. Of course, some reevaluation of these discrepancies or even new measurements will be highly desirable.

Research at the Oak Ridge National Laboratory is supported by the U.S. Department of Energy under Contract No. DE-AC05-96OR22464 with Lockheed Martin Energy Research Corp. We acknowledge also CONACYT, Mexico, Contract Nos. E120.2236 and 3756E, and NSF Contract No. INT-9416288. Oak Ridge Institute for Science and Education is managed by Oak Ridge Associated Universities for the U.S. Department of Energy under Contract No. DE-AC05-76OR00033.

[1] J. Wilczynski, K. Siwek-Wilczynska, J. Van Driel, S. Gonggrijp, D. C. J. M. Hageman, R. V. G. Janssens, J. Lukasiak, R. H. Siemssen, and S. Y. Van Der Werf, Nucl. Phys. **A373**, 109 (1982).

[2] H. Morgenstern, W. Bohne, W. Galster, K. Grabish, and A. Kyanowski, Phys. Rev. Lett. **52**, 1104 (1984).

[3] Y. Chan, M. Murphy, R. G. Stokstad, I. Tserruya, S. Wald, and A. Budzanowski, Phys. Rev. C **27**, 447 (1983).

[4] M. F. Vineyard, Phys. Rev. C **49**, 948 (1994).

[5] A. Chbihi *et al.*, Phys. Rev. C **43**, 652 (1991).

[6] B. B. Back, K. L. Wolf, A. C. Mignerey, C. K. Gelbke, T. C. Awes, H. Breuer, V. E. Viola, Jr., and P. Dyer, Phys. Rev. C **22**, 1927 (1980).

[7] K. A. Griffioen, E. A. Bakkum, P. Decoloski, R. J. Meijer, and R. Kamermans, Phys. Rev. C **37**, 2502 (1988).

[8] B. Faure-Ramstein, F. Auger, J. P. Wieleczko, W. Mittig, A. Cunsolo, A. Foti, E. Plagnol, J. Québert, and J. M. Pascaud, Nucl. Phys. **A586**, 533 (1995).

[9] D. Shapira *et al.*, Nucl. Instrum. Methods Phys. Res. A **301**, 76 (1991).

[10] J. Gomez del Campo *et al.*, Phys. Rev. C **53**, 222 (1996).
[11] J. Gomez del Campo *et al.*, Rev. Mex. Fis. **42-1**, 101 (1996).
[12] D. Shapira, J. Gomez del Campo, M. Korolija, J. Shea, C. F. Maguire, and E. Chavez-Lomeli, Phys. Rev. C **55**, 2448 (1997).
[13] J. Pouliot, Y. Chan, A. Dacal, A. Harmon, R. Knop, M. E. Ortíz, E. Plagnol, and R. G. Stokstad, Nucl. Instrum. Methods Phys. Res. A **270**, 69 (1988).
[14] J. Gomez del Campo and R. G. Stokstad, Report No. ORNL TM-7295 (1981).
[15] M. Blann, Phys. Rev. C **31**, 1245 (1985).
[16] R. Bonetti, M. Camnasio, L. Colli-Milazzo, and P. E. Hodgson, Phys. Rev. C **24**, 71 (1981).
[17] J. Randrup and R. Vandenbosch, Nucl. Phys. **A474**, 219 (1987).
[18] A. D'Onofrio *et al.*, Phys. Rev. C **39**, 834 (1989).